A. Saravanan[1]
Department of Mechanical Engineering,
Aditya Engineering College,
Surampalem, East Godavari 533 437,
Andhra Pradesh, India
e-mail: saravanan.a@aec.edu.in

M. Murugan
Department of Mechanical Engineering,
Aditya College of Engineering & Technology,
Surampalem, East Godavari 533 437,
Andhra Pradesh, India
e-mail: manickam.murugan@acet.ac.in

M. Sreenivasa Reddy
Department of Mechanical Engineering,
Aditya Engineering College,
Surampalem, East Godavari 533 437,
Andhra Pradesh, India
e-mail: srmedapati@aec.edu.in

Pramod Kumar
Department of Mechanical Engineering,
Aditya College of Engineering & Technology,
Surampalem, East Godavari 533 437,
Andhra Pradesh, India
e-mail: pramodkumar@acet.ac.in

P. V. Elumalai
Department of Mechanical Engineering,
Aditya Engineering College,
Surampalem, East Godavari 533 437,
Andhra Pradesh, India
e-mail: elumalai@aec.edu.in

Performance Enhancement of Tubular Solar Still With Various Rotating Wicked Materials—An Experimental Approach

The need for freshwater grows by the day, yet the amount of freshwater accessible worldwide is insufficient to fulfil it. The distillation of saltwater could be a way to meet the demand for freshwater. The current study investigates the experimental performance enhancement of a tubular solar still (TSS) with various rotating wick materials. A rotating drum consisting of multiple wick materials (black bamboo cotton fabric, jute cloth, terry cotton, and polyester) was placed within the tube to increase the evaporation rate. The basin water depth was set at 2 cm to increase the productivity of distillate water. The black bamboo cotton fabric wick outperformed the jute cloth wick, terry cotton wick, polyester wick, and conventional tubular solar still (CTSS) by 5.7%, 12.44%, 19.94%, and 48%, respectively, while maintaining the wicked drum speed around 1 rpm. Because of its moisture-wicking nature, the efficiency of a TSS with a rotating wick made of black bamboo cotton fabric is 50.65% greater than that of a CTSS. Compared with other wick materials, it had a high absorption and evaporation rate. Furthermore, the performance of TSS was investigated, using a black bamboo cotton fabric wicked drum at 0.3, 0.5, 1, 2, and 3 rpm. The studies indicated that a wicked drum speed of 0.5 rpm improves the productivity of approximately 7.474 kg/m^2. Furthermore, the average TSS efficiency was increased by 70.8% compared with the CTSS. [DOI: 10.1115/1.4054071]

Keywords: energy systems, experimental techniques, tubular solar still, heat transfer enhancement

Introduction

Water and energy consumption are two interconnected areas that govern our lives and shape society. The most significant problem affecting many parts of the world is the difficulty to provide sufficient quantities of high-quality freshwater for drinking, particularly in arid and remote places [1]. The amount of saltwater accounts for approximately 97.5% of water accessible on the Earth's surface. As a result, the freshwater content is around 2.5%. However, most of this freshwater is trapped in ice caps and underground subterranean reservoirs. Nowadays, salty or brackish water desalination is a standard method of producing freshwater. Desalination decreases the salinity of saltwater from a higher concentration of dissolved particles to less than 300 ppm, which is considered acceptable. Several ways are used to convert saltwater into safe freshwater. Ahsan et al. [2] conducted a comparative evaluation of modified tube stills and traditional solar stills. Chen et al. [3] have found that the desalination water yield and efficiency depended on temperature, relevant dimensions of the still, pressure, and input power. Porta-Gándara et al. [4] have increased freshwater productivity by injecting air bubbles to disturb the basin water. Zanganeh et al. [5] have enhanced the productivity by coating different nanoparticles in the glass cover. By adding the nanoparticles to the glass cover, the wettability of the condensation surface enhances the distillate water output. The result shows that the silicone Nano coating enhances the productivity of solar still (SS) by 20% than without coating. Abdullah et al. [6] created a multi-tray solar still with a reflector to boost evaporation. They discovered that the modified solar still outperforms the regular solar by 95%.

Jahanpanah et al. [7] utilized a PCM (low-temperature) solar still with a single slope to achieve a longer desalination process. The results reveal that PCM increased the total production by 30.3% compared with conventional. Kabeel et al. [8] investigated the effect of solar stills (pyramid-shaped) with hollow circular fins and PCM. They discovered that PCM in a finned water basin increased yield by around 101.5% above conventional methods. Mohamed et al. [9] demonstrated a 123% improvement in the exergy efficiency of a porous absorber CSS with a 2 cm fine stone. Shehata et al. [10] designed an ultrasonic humidifier with an evacuated solar collector in single slope solar still to enhance productivity. With a water depth of 35 mm, the modified solar still boosted the productivity by 45% compared with a conventional solar still (CSS). Fallahzadeh et al. [11] increased production by combining a working medium of water and ethanol with an integrated heat pipe. They discovered that using water as a working fluid at a 40% filling ratio resulted in a 111.2% improvement in freshwater yield than a typical solar still. Amiri et al. [12] conducted an experimental and theoretical investigation of a solar still combined with a parabolic trough collector. The experimental results reveal that production was increased by 55% during the summer session compared with the winter session. Younis et al. [13] improved freshwater production by adapting a standard solar still and integrating it with a revolving drum. The results show that a rough spinning drum with a radius to length ratio of 24.5 provides about 431.1% more production than a solar still without a drum.

Saravanan and Murugan [14] investigated the evaporation rate of square pyramid solar still with different wick materials by changing the basin water depth. A solar still with woollen wick material and a

[1]Corresponding author.

Manuscript received October 21, 2021; final manuscript received February 23, 2022; published online April 7, 2022. Assoc. Editor: Cheng-Xian Lin.

water level of 2 cm produced a maximum production of 5.8 kg/m^2, which was 40.3% higher than a typical sun still. Murugan et al. [15] investigated the performance of a wick-type solar still combined with a V-trough solar water heater. They determined that compared with the traditional approach, the productivity of the modified solar still using fur fabric material increased by 30.12%. Dumka et al. [16] conducted an experimental and theoretical study to enhance freshwater yield by introducing jute-covered plastic balls to the water basin. They discovered that when compared with standard solar still, the modified solar still improves overall thermal efficiency by 32.76%. Murugan et al. [17] published a comprehensive study of solar stills utilizing wick materials. Alshammari et al. [18] conducted a techno-economic feasibility study and evaluated the use of multi-effect tubular solar still. Yan et al. [19] studied the vapor transportation of tubular solar still working under vacuum and discovered that for operating pressure values smaller than 60 kPa, the water productivity rate improved by more than 50%.

Kabeel et al. [20] enhanced tubular solar still performance using hybrid storage materials and a Compound Parabolic Collector. The results show that the output of distillate water rose by 65.4% compared with the traditional approach. Kabeel et al. [21] modified the structure of the tubular solar still by adding two semi concentric cylinders and tubular parabolic concentrators within and outside the solar still, respectively, to increase the productivity of the distillate water. According to the data, the modified tubular solar still generated 90.8% more than the standard. Sathyamurthy et al. [22] studied the addition of fins on the absorber plate surface to increase the evaporation rate by heating the basin water. The results showed that the solar still production was 46.85% higher than conventional. Abdelgaied et al. [23] used vertical and inclined pin fins in tubular solar still combined with an external condenser. Compared with a typical solar still, fins and a condenser increased production by 71.6%. By maintaining the PCM material in the water basin, Kabeel et al. [24] conducted an experimental investigation of tubular solar still to get freshwater productivity during the day and night. Compared with traditional still, the basin with PCM material increases freshwater production by 115.1%. In an experimental investigation of tubular solar stills, Kabeel et al. [25] utilized graphene oxide nanoparticles in PCM to improve freshwater output by 41.3%.

Tiwari and Kumar [26] invented and theoretically tested the tubular solar still. Kabeel et al. [27] examined the effect of water depth and tubular surface cooling methods on tubular solar still performance. They observed a water depth of 0.5 cm and a cooling water flowrate of 2 l/h increased the efficiency by 54.9%. Abdullah et al. [28] explored the impact of trays solar stills through corrugated wick absorbers and nano-enhanced phase change material on freshwater production. The results showed that the modified solar still outperformed the standard solar still in terms of production by 180%. Abdelgaied et al. [29] studied the productivity of tubular solar stills by keeping a PCM reservoir in square and circular hollow finned water basins. They concluded that the circular fin with PCM reservoir solar still increased freshwater output by 90.1%. Kumar and Anand [30] studied the impact of wick in tubular solar still to increase distillate yield by more than 18% compared with conventional. Kabeel et al. [31] increased productivity by utilizing wick materials to provide a V-corrugated absorber surface. They observed that TSS with a v-corrugated absorber plate and wick materials beats a traditional by 44.82%.

Abdullah et al. [32] utilized a rotating drum inside the solar still basin, a condenser, and nanoparticles to enhance productivity by increasing evaporative surface area and decreasing saline water layer thickness. They determined that the modified solar still outperformed the standard solar still in terms of freshwater productivity by 350%. Essa et al. [33] improved the tubular solar still by including a rotating drum with a shallow basin. The evaporative heat transfer was enhanced by keeping the rotating drum inside the TSS. The influence of productivity was further studied by maintaining the drum at various rotating speeds. The results exposed that increasing the speed of a TSS without wick by 0.1 rpm improved yield by 140% and 175%, respectively, and thermal efficiency was 56.4% and 61% for closed ends and open ends drums.

According to prior research, no experiments on the performance of TSS with rotating wick to improve its performance have been conducted. As a result, the primary goal of the current experimental study is to explore the TSS with a wicked rotating drum to improve

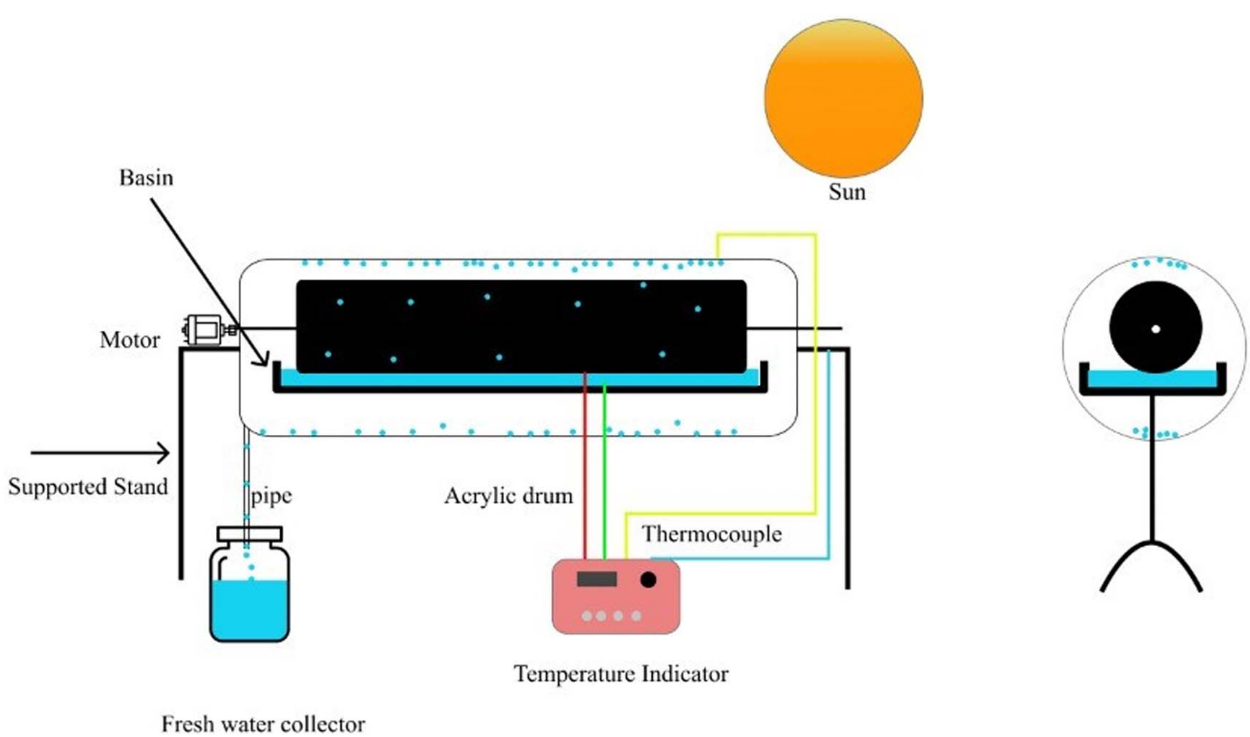

Fig. 1 Experimental setup schematic diagram

Fig. 2 A visual representation of the experimentation setup

still performance by boosting the evaporation rate. Two experimental methods were examined to test this hypothesis. In the first experimental scenario, the effects of different wick materials (polyester, terry cotton, jute, and black bamboo cotton) were investigated to identify the ideal wick material for the most significant freshwater production while keeping the wicked drum speed around 1 rpm. In the second experimental scenario, the influence of black bamboo cotton fabric drum speeds (0.3, 0.5, 1, 2, and 3 rpm) on TSS performance was investigated.

Experimental Setup

The present experimental setup was created to support two separate practical scenarios. The influence of using various rotating wick (black bamboo cotton fabric, jute cloth, terry cotton, and polyester) drums at a drum speed of 1 rpm was examined in the first scenario. The second scenario was used to investigate the effect of a rotating drum made of black bamboo cotton fabric that rotated at different speeds (0.3, 0.5, 1, 2, and 3 rpm). As seen in Figs. 1 and 2, a transparent polycarbonate cylinder allows solar irradiation to penetrate from any direction. The polycarbonate tube is 62 cm in length, 50 cm in diameter, and 5 mm in thickness. The rectangular water basin is made of copper sheet and is 60 cm long, 43 cm wide, and 8 cm high. The basin's top and bottom were painted black mud to absorb as much sun heat rays as possible. The basin is supported in the middle of the polycarbonate tube.

Specifications of Wick Materials. Tubular solar still's daily output has increased due to decreased volumetric heat capacity (VHC). The VHC was reduced, and the evaporation rate of basin water was increased by retaining the wick material within the TS. Wick materials are chosen depending on porosity, absorbency, water vapor permeability, heat transfer coefficient, and gram per square meter (GSM) characteristics.

Absorbency. Water absorbency is the rate at which water is taken into and morphed into another object or phase. Water can be absorbed into the atmosphere and change into another state, such as gas, or absorbed into an object, like a sponge. Different fibers thus absorb different amounts of water.

Porosity. Porosity is a measure of the void (i.e., "empty") spaces in a material and is expressed as a percentage of the volume of voids over the entire volume, ranging from 0 to 100%

$$\varnothing = \frac{\text{Pore Volume } (V_p)}{\text{Bulk Volume } (V_b)}$$

Pore volume (V_p):

Pore volume may be determined by the fluid saturation method (material immersed in water)

$$W_{\text{water}} = W_{\text{sat}} - W_{\text{dry}}$$

$$V_p = \frac{W_{\text{water}}}{\rho_{\text{water}}}$$

Bulk volume (V_b):

Bulk volume may be determined by linear measurement value (dimension of the wick material)

$$V_b = \text{length} \times \text{breath} \times \text{thickness}$$

Water Vapor Permeability. Water vapor permeability is defined as a fabric's ability to transport water vapor from the fabric to the external environment. Materials with a high permeability allow easy flow, while materials with a low permeability resist flow.

Heat Transfer Coefficient. The evaporative heat transfer coefficient, a function of the heat transfer coefficient between the wet wick absorber surface and the glass cover, governs water evaporation within the still. The temperature differential determines the heat transfer coefficient between the absorber and the glass cover and the difference in partial pressure of water vapor between the wick absorber and the glass cover.

The heat transfer between the wet wick absorber and the glass cover can be given as

$$h = \frac{q}{\Delta T}; \quad \Delta T = T_w - T_g$$

Capillary Rise. Capillary rise is the rise in pressure of a liquid above zero due to a net upward force created by the attraction of water molecules to a solid surface, such as glass, fabric, or dirt. The capillarity of wick materials may be determined using a typical vertical wicking test procedure. Table 1 lists the parameters for each wick material. The performance of the TSS with rotating wicked drum materials such as black bamboo cotton fabric, jute cloth, terry cotton, and polyester cloth was investigated in this study. Figure 3 illustrates the various wick materials used in this study. The wicked rotating drum was built from different wick materials and had a 600 mm × 530 mm size coved above the cylindrical frame (190 mm × 530 mm) made from a mild steel rod. The wicked rotating drum was mounted on a rotating rod supported by two bearings. A direct current motor (12 W) rotated the drum.

Table 1 Material specifications for the wick

Types of wick	Porosity (%)	Absorbency (sec)	Water vapor permeability (gram/h · m^2)	Heat transfer coefficient (W/m^{2}K)	GSM (gram/m^2)
Black bamboo cotton fabric	24.5	3	19.2	58.4	220
Jute cloth	25.3	9	4.9	15.4	521.6
Terry cotton	22.6	23	10.2	36	216.6
Polyester cloth	16.8	41	14.1	28	142.3

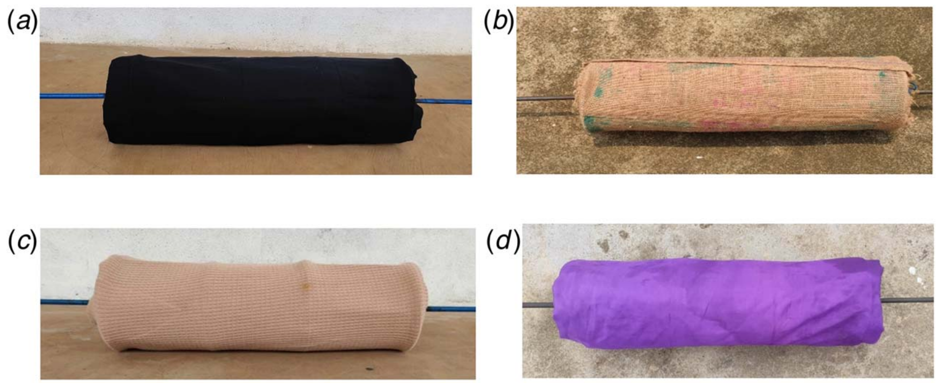

Fig. 3 Wicked drum with different wick materials: (*a*) black bamboo cotton fabric, (*b*) jute cloth, (*c*) terry cotton, and (*d*) polyester cloth

A DC controller, which was connected to the direct current motor, controlled the rotating speed of the wicked drum.

Experimental Procedure and Instrumentation. TSS was planned, built, and tested on the roof of the department building at Aditya Engineering College in Surampalem, Andhra Pradesh, India (17.0814 deg N latitude and 82.05 deg E longitude) during clear sunny days in April and May 2021. From 8.30 am to 6 pm, average basin temperature (T_b), basin water temperature (T_w), mean glass cover temperature (T_g), ambient temperature (T_a), the solar intensity $I(t)$, average air velocity (V), and freshwater productivity (m_w) were monitored once every half hour. The saltwater utilized in this experiment is seawater obtained at Kakinada, India, from the Bay of Bengal. Feeding the compensatory feed saltwater tank fills the water basin with a set depth of 2 cm [14]. T_w was measured with two T-type thermocouple wires floating in the basin water, whereas T_g was measured with four wires mounted on the polycarbonate tube at four different places. A T-type thermocouple was welded at six different positions in the copper basin to measure T_b. All thermocouple cables wires were connected to a digital thermometer. From 8.30 am to 6 pm, sun intensity $I(t)$, average air velocity (V), and freshwater productivity (m_w) were recorded every half hour. The solar intensity was measured with a solar meter with a 1 W/m^2 resolution. V was measured with a hotwire anemometer with a 5% accuracy.

The productivity of distilled water was measured using a 2 l flask with a precision of 5 ml. Equations (1) and (2) are used to calculate the uncertainty of the equipment used in this study to measure the solar irradiation, temperature, wind velocity, TDS, pH value, electrical conductivity, and accumulated distillate. Table 2 displays the measuring instrument parameters with the standard uncertainty. The standard uncertainty of the measuring equipment was represented as follows [34]:

$$\text{Standard uncertainty } (u) = \frac{\text{Accuracy of the instrument } (a)}{\sqrt{3}} \tag{1}$$

The experimental measurements are used to calculate some desired results of the experiment (R). Thus

$$R = R(x_1, x_2, x_3, \ldots\ldots\ldots\ldots, x_n)$$

The uncertainty in the result is calculated as follows:

$$u = \left[\left(\frac{\partial R_1}{\partial X_1}u_1\right)^2 + \left(\frac{\partial R_2}{\partial X_2}u_2\right)^2 + \left(\frac{\partial R_3}{\partial X_3}u_3\right)^2 + \cdots + \left(\frac{\partial R_n}{\partial X_n}u_n\right)^2\right]^{0.5} \tag{2}$$

where u is the uncertainty in the result, n is the number of experimental variables and $u_1, u_2, \ldots, u_n$ are the uncertainties in the independent variables ($x_1, x_2, \ldots\ldots$ and x_n).

The measurement instruments' standard uncertainty was represented as follows. The total uncertainty based on performance is determined using the collected distillate, and the solar intensity falling on the slanted surface is mathematically expressed as Eq. (3)

$$u(\eta_d) = \left[\left(\frac{\partial \eta_d}{m_w}u_{m_w}\right)^2 + \left(\frac{\partial \eta_d}{I(t)}u_{I(t)}\right)^2 + \left(\frac{\partial \eta_d}{h_{fg}}u_{hfg}\right)^2 + \left(\frac{\partial \eta_d}{A}u_A\right)^2\right]^{0.5}$$

$$u(\eta_d) = \partial \eta_d\left[\left(\frac{u_{m_w}}{m_w}\right)^2 + \left(\frac{u_{I(t)}}{I(t)}\right)^2 + \left(\frac{u_{hfg}}{h_{fg}}\right)^2 + \left(\frac{u_A}{A}\right)^2\right]^{0.5} \tag{3}$$

The amount of freshwater collected determines the uncertainty of the distillate collected in the flask, which is expressed as Eq. (4)

$$u_m = \left[\left(\frac{\partial m}{\partial m_w}u_{m_w}\right)^2\right]^{0.5} \tag{4}$$

where η_d, m_w, $I(t)$, h_{fg}, and A are the cumulative efficiency, mass of distillate, solar intensity on glass surface, latent heat of water, and

Table 2 Specifications of the measuring instrument with parameter

Instrument	Range	Accuracy	Standard uncertainty
Solar power meter	0–1999 W/m^2	±1 W/m^2	±0.57 W/m^2
Hotwire anemometer	0.1–18 m/s	±0.1 m/s	±0.057 m/s
T type thermocouple	0–200 °C	±0.5 °C	±0.29 °C
TDS meter	0–4999 ppm	±1 ppm	±0.57 ppm
pH meter	0–14	±0.01 pH	±0.0057 pH
Water conductivity meter	0–9.999 mS/m	±0.001 mS/m	±0.00057 μS
Measuring jug	0–1000 ml	±5 ml	±2.9 ml

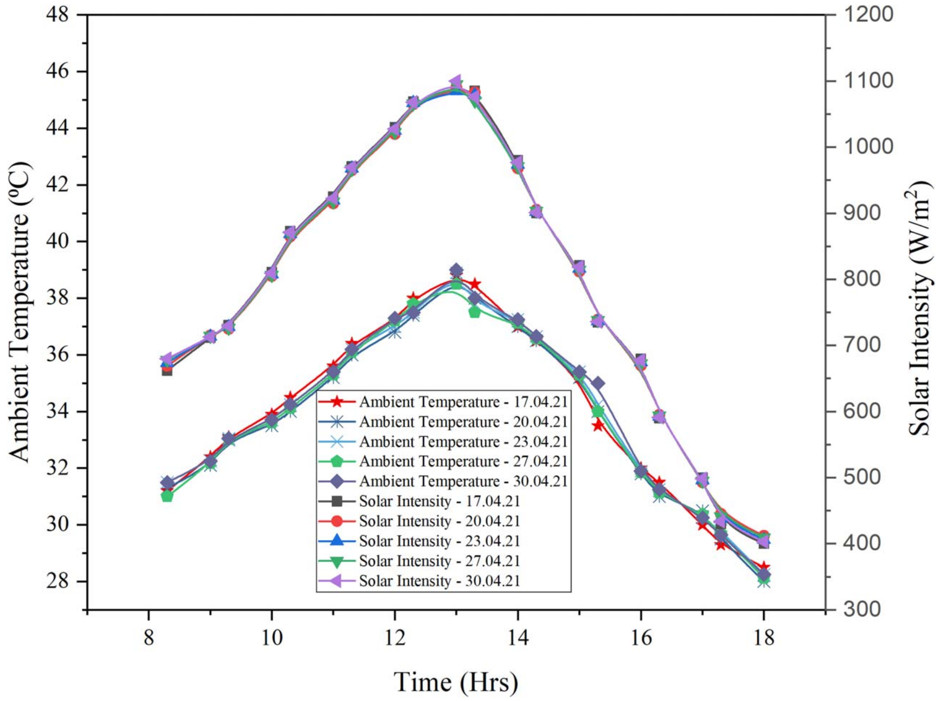

Fig. 4 Variation in solar intensity and ambient temperature on trial days

water basin area. Based on the independent variables, the uncertainty of the systems is expressed as

$$u = u_1 + u_2 + u_3 + \cdots + u_n \tag{5}$$

where u represents the overall uncertainty of the system and u_1, u_2, u_3, …, u_n represents the uncertainty of the individual independent variable. Using Eqs. (4) and (5), the maximum uncertainty of cumulative efficiency and amount of freshwater collected for the TSS with the black bamboo cotton wicked drum was calculated to be 6.73% and 0.84%, respectively.

Solar Still Efficiency. Tubular solar still efficiency was generally determined by the combined effect of hourly distillate water

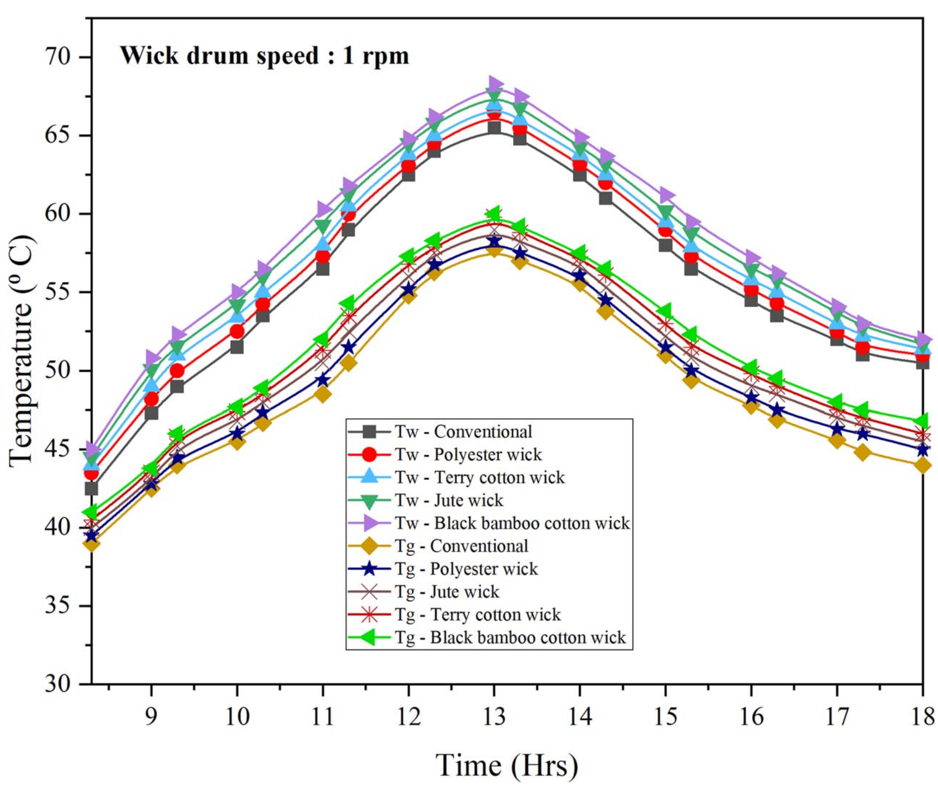

Fig. 5 Variation in basin water and glass cover temperature between proposed and CTSSs

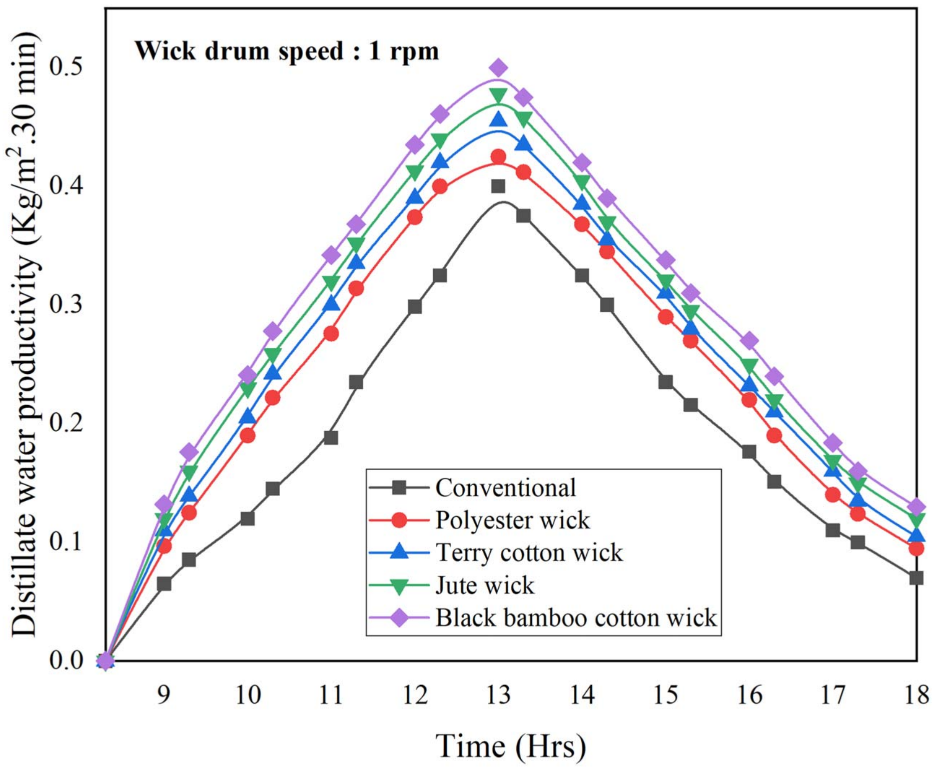

Fig. 6 Variation in distillate water productivity between proposed and CTSSs

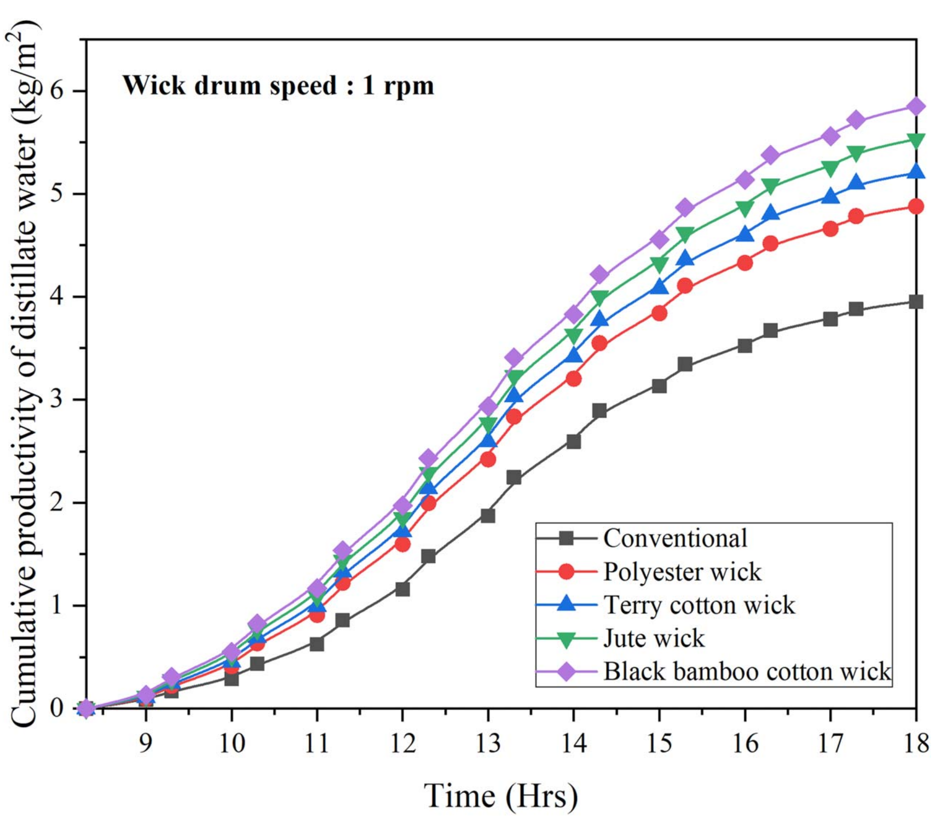

Fig. 7 Variation of cumulative productivity of proposed and CTSSs

productivity, latent heat of basin water, water basin area, and solar intensity, as follows:

$$\eta_d = \frac{m_{ev} \times h_{fg}}{I(t) \times A \times t} \tag{6}$$

Result and Discussion

Effect of Rotating Drum With Different Wick Materials. The productivity of TSS mainly depends on solar intensity, ambient temperature, wind velocity, and design configuration of TSS. The solar intensity throughout the day will provide energy to operate the TSS. The TSS design arrangement (rotating wicked drum) had increased the evaporation rate, resulting in maximum distillate water productivity. The solar intensity and ambient temperature were measured for the experimental trial days. Figure 4 depicts solar intensity and ambient temperature fluctuation throughout a trial day. There were five experimental testing days (17 April, 20 April, 23 April, 27 April, and 30 April). The acquired ambient temperatures ranged from 29 to 39 °C, 28 to 39.5 °C, 28.5 to 40 °C, 28 to 38.5 °C, and 29.5 to 39 °C, while the maximum solar intensity was 1092, 1090, 1085, 1095, and 1100 W/m^2 throughout the five trial days. The ambient temperature range and solar intensity on each of the five testing days are roughly identical.

Figure 5 depicts the variance in basin water and glass temperature of the conventional and proposed TSSs. The rotating wicked drum speed was kept constant at 1 rpm for reference. Both the basin water temperature and the glass temperature increased with time, reaching a peak at 1.00 pm and then decreasing owing to a reduction in sun intensity after that. At 1.00 pm, the maximum basin water temperature for black bamboo cotton fabric, jute cloth, terry cotton, polyester, and traditional TSS is 68.5, 68, 67, 66.5, and 65.5 °C, respectively. Because of the greater quantity of produced vapor content within the tubular drum still, the proposed TSS glass temperature for all wicked drums was higher than the traditional still. At 1.00 pm, the maximum tubular glass temperature for black bamboo cotton fabric, jute cloth, terry cotton, polyester, and CTSS was 60, 59.5, 58.5, 58, and 57.5 °C respectively.

Figure 6 shows that the distillate water productivity of the suggested TSS was higher than that of the CTSS in all situations. The distillate water output increased over time and decreased due to solar intensity. Figure 6 shows that the maximum distillate water production of black bamboo cotton fabric, jute cloth, terry cotton, polyester, and CTSS are 500 ml, 478 ml, 455 ml, 425 ml, and 400 ml at 01.00 pm for 1 rpm wicked drum speed, respectively. Bamboo cotton fabric can absorb three times more water than its weight, which means getting rid of moisture faster, due to the higher absorbance and evaporation (moisture management properties) [35] nature of black bamboo cotton fabric material.

Additionally, the rotation of the wicked drum produces a thin layer of film of water over the wick. Furthermore, rotating the drum causes turbulence in the flow of fluids (air and water) within the TSS. Figure 7 depicts the difference in cumulative productivity between the proposed and CTSSs. Wicked drum productivity with black bamboo cotton fabric, jute cloth, terry cotton, polyester, and CTSS is 5.85, 5.53, 5.203, 4.877, and 3.95 kg/m^2, respectively. The results show that when using the wicked drum material as black bamboo cotton fabric, jute cloth, terry cotton, and polyester, the cumulative productivity increased by 48.1%, 40%, 31.7%, and 23.5%, respectively, as compared with the CTSS.

Figure 8 depicts the solar still efficiency of a conventional and proposed TSS with various rotating wicked drums. The solar still efficiency of CTSS is usually lower than that of the proposed TSS with different rotating drums with wick material. The solar still efficiency of the proposed wicked drum TSS with black bamboo cotton fabric, jute cloth, terry cotton, and polyester materials ranged between 12.22 and 30%, 11.1 and 28.2%, 10.2 and 26.9%, and 9 and 25.2%, respectively, whereas the CTSS was between 5.2 and 23.4%.

During the trial days from 8.30 am to 6 pm, the average still efficiency of the proposed wicked drum TSS with black bamboo cotton fabric, jute cloth, terry cotton, polyester, and conventional was 24.07, 22.7, 21.27, 19.9, and 15.8%, respectively. This study demonstrates that using bamboo cotton fabric wicked drum in TSS increases average efficiency by 5.6, 13.4, 20.9, and 51.5%, respectively, compared with jute cloth, terry cotton, polyester, and CTSS.

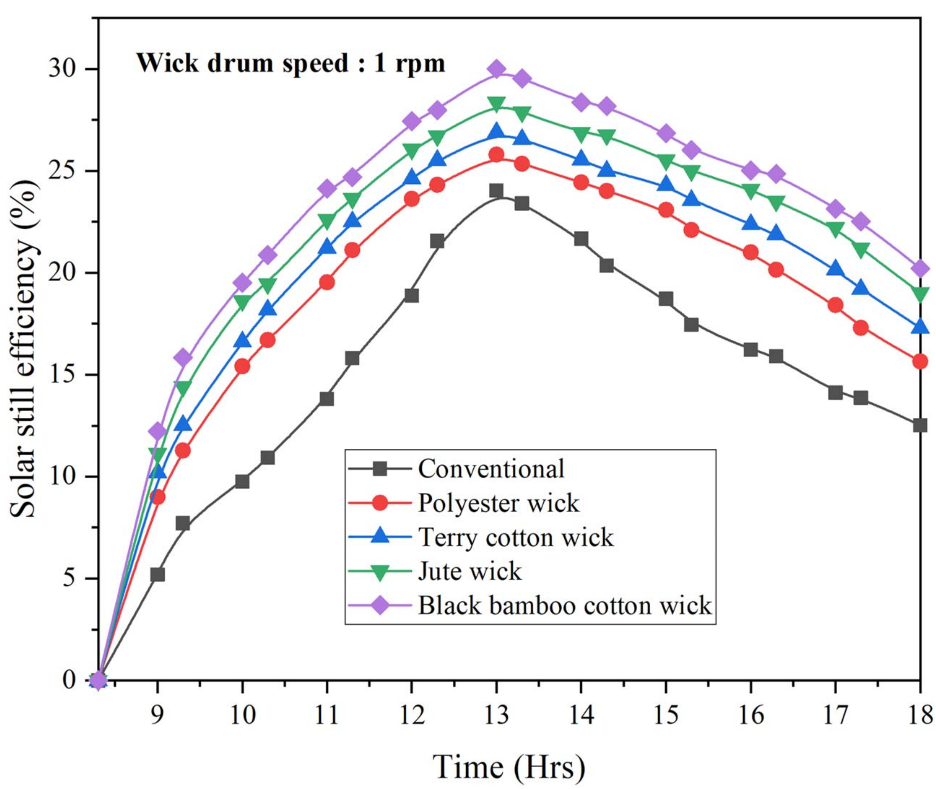

Fig. 8 Variation of solar still efficiency of proposed and CTSSs

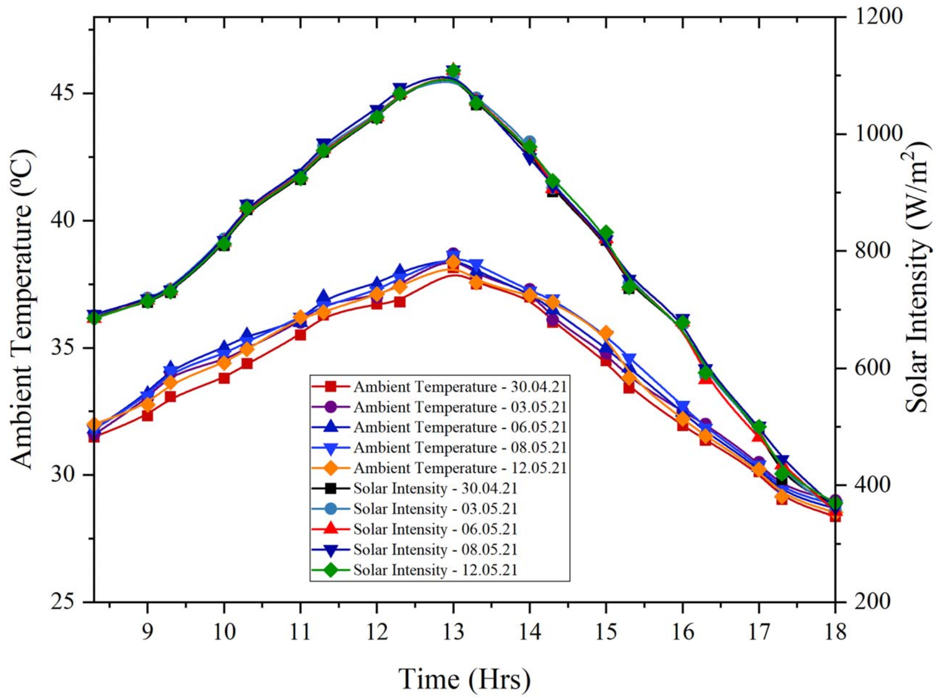

Fig. 9 Variation of solar intensity and ambient temperature of experimental trial days for black bamboo cotton fabric wicked drum TSS

Effect of Black Bamboo Cotton Fabric Drum With Different Speed. According to the first study, black bamboo cotton fabric wicked drum utilization outperformed other wick materials. The solar intensity and ambient temperature of the five preceding days (30 April, 3 May, 6 May, 8 May, and 12 May) exhibit identical behavior. Figure 9 depicts solar intensity and ambient temperature variation throughout a trial day. The ambient temperatures were between 28.5 and 38 °C, 29 and 39 °C, 28.5 and 38.5 °C, 28.5 and 39 °C, and 28.5 and 38 °C, while the highest solar intensity was 1108, 1100, 1109, 1110, and 1108 W/m^2 across the five testing days.

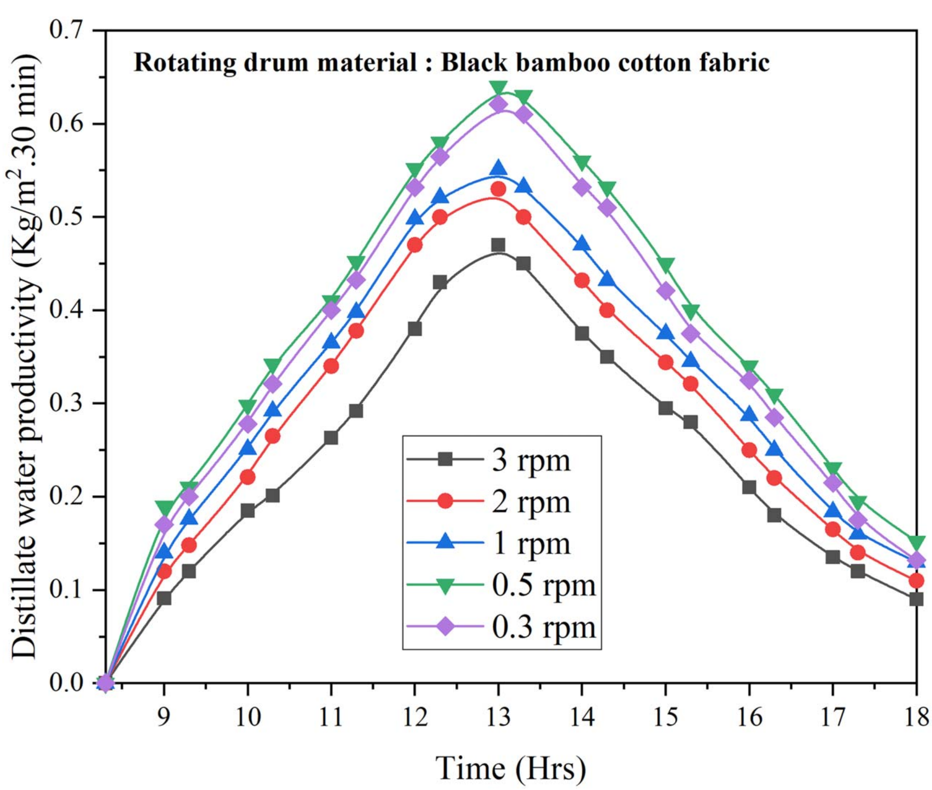

Fig. 10 Variation of distillate water productivity for different rotating speeds of black bamboo cotton fabric wicked drum

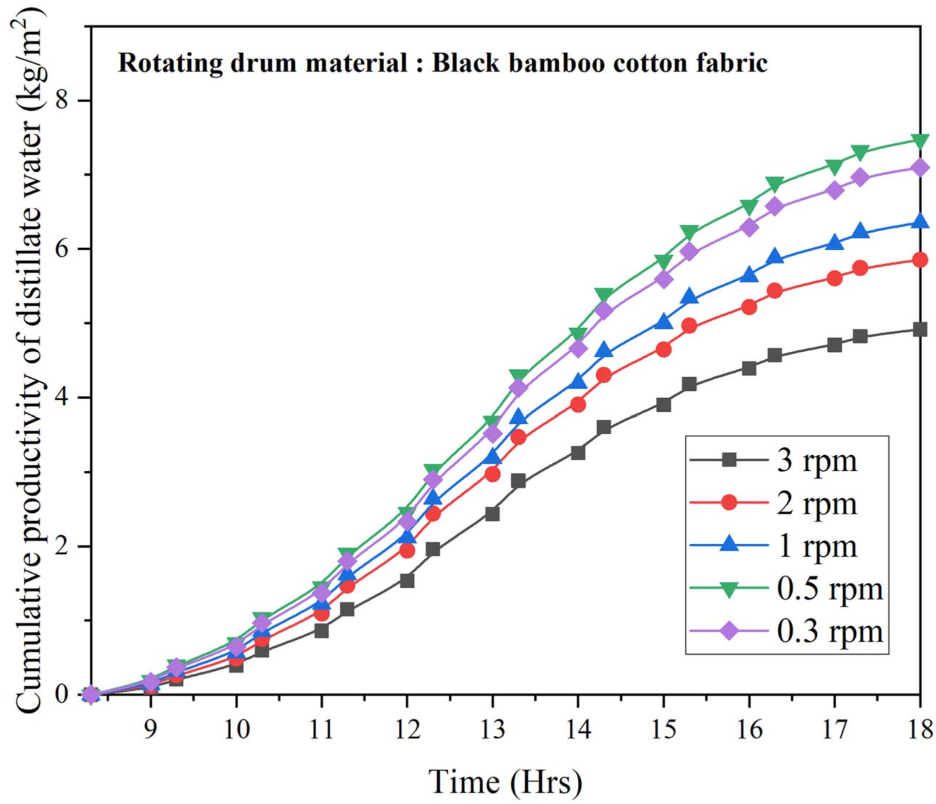

Fig. 11 Variation of cumulative water productivity for different rotating speeds of black bamboo cotton fabric wicked drum

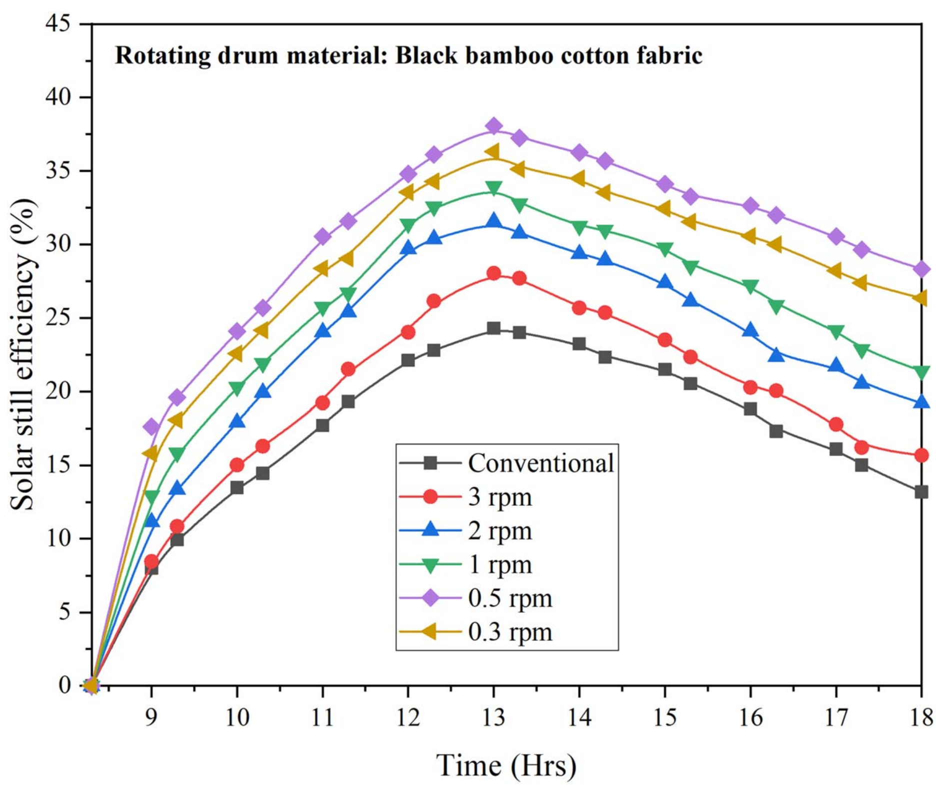

Fig. 12 Variation of solar still efficiency for different rotating speeds of black bamboo cotton fabric wicked drum

Table 3 Comparison among the different studies of solar still with our present TSS

Researcher	Modifications proposed	Cumulative productivity, kg/m^2 · day	Present TSS with rotating wicked drum, kg/m^2 · day	Increase in productivity %
Abdelgaied et al. [23]	TSS with pin fins and external condenser	5.94	7.474	25.82
Essa et al. [33]	TSS using a rotating drum	6.6	7.474	13.24
Kabeel et al. [27]	TSS by varying water depth and cover cooling	5.85	7.474	27.8
Saravanan and Murugan [14]	SS with different vertical wick materials	5.636	7.474	32.61
Murugan et al. [15]	SS with a V-trough solar water heater	6.29	7.474	18.9
Dumka et al. [16]	SS with jute-covered plastic balls	2.426	7.474	208

Table 4 Characteristics of the sample (seawater) and distillate water

Characteristics	Sample water (seawater)	Distillate water output	WHO drinking-water quality guidelines	Standard testing method
Total dissolved solids, ppm	1183	43	<600	ASTM D5907-18
*p*H value	8.6	7.3	6.5–8	ASTM D1293-18
Electrical conductivity, S/m	4.1	0.0094	0–0.08	ASTM D1125-14

Figure 10 depicts the change in distillate water productivity for different rotating speeds of a wicked drum made of black bamboo cotton cloth. TSS with black bamboo cotton fabric wicked drum produced 621 ml, 640 ml, 551 ml, 530 ml, and 470 ml of distillate water at drum speeds of 0.3, 0.5, 1, 2, and 3 rpm. The effective speed of the wicked rotating drum was determined to be 0.5 rpm based on the results. The absorption and evaporation rates were nearly identical at 0.5 rpm wicked drum speed. The productivity of freshwater decreased after the effective speed because the absorption rate of the wick was more significant than the evaporation rate, even if the turbulence of the basin water was considerable.

Furthermore, the value below the effective speed reduces freshwater productivity since the absorption rate is lower than the evaporation rate. Figure 11 depicts the cumulative productivity of a black bamboo cotton fabric wicked drum with varying rotating speeds. The findings showed that at 6 pm, the quantity of collected distillate water for the 0.5 rpm speed was around 7474 ml/m^2, while the comparable figures for the 0.3, 1, 2, and 3 rpm were almost 7099, 6357, 5854, and 4917 ml/m^2, respectively. From the above findings, the cumulative productivity of a black bamboo cotton fabric wicked drum with a speed of 0.5 rpm increased by roughly 5.27%, 17.57%, 27.67%, and 52%, respectively, compared with speeds of 0.3, 1, 2, and 3 rpm. The suggested TSS increases freshwater productivity by 89.14% more than the CTSS.

Figure 12 depicts the variation in solar still efficiency for different rotational speeds of a wicked drum made of black bamboo cotton cloth. The solar still efficiency was estimated using the findings of Figs. 10 and 9. According to the results, the TSS with bamboo cotton fabric wicked drum at 0.5 rpm provides the highest still efficiency compared with the remaining speed. The still efficiency of TSS with bamboo cotton fabric wicked drum at 0.5 rpm ranged between 17.62 and 38.08%, whereas at 0.3, 1, 2, and 3 rpm ranged between 15.8 and 36.32%, 12.95 and 33.95%, 11.14 and 31.57%, and 8.46 and 28.04%, respectively. The average solar still efficiency from 9:00 a.m. to 6:00 p.m. was 30.91%, 29%, 26.12%, 23.89%, and 20.22% with wicked drum speeds of 0.5, 0.3, 1, 2, and 3 rpm, respectively. According to these data, using a bamboo cotton fabric wicked drum at a speed of 0.5 rpm improves the average efficiency of the CTSS by 70.8%.

Comparison Summaries of Current Tubular Still Designs. Table 3 compared the present study's findings with the findings of another previous study's other arrangement. The comparisons reveal that our proposed TSS suggested in this study is the optimum alteration for improving TSS performance. This comparison seeks to demonstrate the benefits of the current TSS modification over the prior study.

Quality of Water Testing. To achieve the intended aim of the water desalination technique, the authors analyzed a water sample before and afterward the distillation process in terms of *p*H and TDS. The study results indicated that the TDS levels before and after the desalination procedure were 1183 and 43 ppm, respectively. The *p*H value decreased from 8.6 to 7.3, and the electrical conductivity reduced from 4.1 S/m to 0.0094 S/m. As a result, the output distillate water quality was determined to be within the World Health Organization's (WHO) [36] permitted limit. The characteristics of the sample (seawater) and distillate water are shown in Table 4.

Conclusion

The present experiment was aimed to improve the TSS by keeping the wicked rotating drum with different wick materials. The proposed TSS was compared with the CTSS. Furthermore, the performance of the proposed TSS was tested at various rotational speeds of the drum. The most significant outcomes are listed as follows:

- For a CTSS, the accumulated distillate reached 3951 ml/m^2. However, the collected distillate for the proposed rotating wicked drum TSS was 5.850, 5.530, 5.203, and 4.877 kg/m^2 for black bamboo fabric, jute, terry cotton, and polyester, respectively.
- Compared with CTSS, the proposed TSS with black bamboo cotton wicked drum increased cumulative output by 48%.
- The solar still efficiency of the proposed TSS with a rotating wick made up of black bamboo cotton fabric is 50.65% greater than that of a CTSS.
- Furthermore, the performance of TSS was studied at various drum rotational speeds (3, 2, 1, 0.5, and 0.3 rpm). Compared with a CSS, the black bamboo cotton wicked drum TSS at 0.5 rpm improved accumulated productivity to 7.474 kg/m^2 · day, representing an 89.2% increase in productivity.

- Compared with CSS, the proposed TSS with a bamboo cotton wicked drum at 0.5 rpm improved daily efficiency by 70.8%.
- According to the data, the TSS with a black bamboo cotton wicked drum at 0.5 rpm is a suitable alternative for achieving the best TSS performance.

Conflict of Interest

There are no conflicts of interest.

Data Availability Statement

The authors attest that all data for this study are included in the paper.

Nomenclature

A = water basin area, m^2
V = wind velocity, m/s
h_{fg} = latent heat of vaporization, J/kg
m_b = mass of the basin, kg
m_d = daily distillate water productivity, kg/(m^2day)
m_{ev} = hourly distillate water productivity, kg/(m^2h)
m_w = mass of water in the basin, kg
T_a = ambient temperature, °C
T_b = basin temperature, °C
T_g = average glass temperature, °C
T_w = average basin water temperature, °C
$I(t)$ = solar intensity, W/m^2

Greek Symbols

η = overall thermal efficiency, %
Φ = porosity of wick material, %

Subscripts

a = ambient
b = basin
g = glass cover
w = basin water

References

[1] Moukhtar, I., El Dein, A. Z., Elbaset, A. A., and Mitani, Y., 2021, *Solar Energy Technologies, Design, Modeling, and Economics*, Springer, New York.
[2] Ahsan, A., Shafiul Islam, K. M., Fukuhara, T., and Ghazali, A. H., 2010, "Experimental Study on Evaporation, Condensation and Production of a New Tubular Solar Still," Desalination, **260**(1–3), pp. 172–179.
[3] Chen, Z., Yao, Y., Zheng, Z., Zheng, H., Yang, Y., Hou, L., and Chen, G., 2013, "Analysis of the Characteristics of Heat and Mass Transfer of a Three-Effect Tubular Solar Still and Experimental Research," Desalination, **330**, pp. 42–48.
[4] Porta-Gándara, M. A., Fernández-Zayas, J. L., and Chargoy-del-Valle, N., 2020, "Solar Still Distillation Enhancement Through Water Surface Perturbation," Sol. Energy, **196**, pp. 312–318.
[5] Zanganeh, P., Goharrizi, A. S., Ayatollahi, S., Feilizadeh, M., and Dashti, H., 2020, "Efficiency Improvement of Solar Stills Through Wettability Alteration of the Condensation Surface: An Experimental Study," Appl. Energy, **268**, p. 114923.
[6] Abdullah, A. S., Younes, M. M., Omara, Z. M., and Essa, F. A., 2020, "New Design of Trays Solar Still With Enhanced Evaporation Methods—Comprehensive Study," Sol. Energy, **203**, pp. 164–174.
[7] Jahanpanah, M., Sadatinejad, S. J., Kasaeian, A., Jahangir, M. H., and Sarrafha, H., 2021, "Experimental Investigation of the Effects of Low-Temperature Phase Change Material on Single-Slope Solar Still," Desalination, **499**, p. 114799.
[8] Kabeel, A. E., El-Maghlany, W. M., Abdelgaied, M., and Abdel-Aziz, M. M., 2020, "Performance Enhancement of Pyramid-Shaped Solar Stills Using Hollow Circular Fins and Phase Change Materials," J. Energy Storage, **31**, p. 101610.
[9] Mohamed, A. F., Hegazi, A. A., Sultan, G. I., and El-Said, E. M. S., 2019, "Augmented Heat and Mass Transfer Effect on Performance of a Solar Still Using Porous Absorber: Experimental Investigation and Exergetic Analysis," Appl. Therm. Eng., **150**, pp. 1206–1215.
[10] Shehata, A. I., Kabeel, A. E., Khairat Dawood, M. M., Elharidi, A. M., Abd_Elsalam, A., Ramzy, K., and Mehanna, A., 2020, "Enhancement of the Productivity for Single Solar Still With Ultrasonic Humidifier Combined With Evacuated Solar Collector: An Experimental Study," Energy Convers. Manage., **208**, p. 112592.
[11] Fallahzadeh, R., Aref, L., Gholamiarjenaki, N., Nonejad, Z., and Saghi, M., 2020, "Experimental Investigation of the Effect of Using Water and Ethanol as Working Fluid on the Performance of Pyramid-Shaped Solar Still Integrated With Heat Pipe Solar Collector," Sol. Energy, **207**, pp. 10–21.
[12] Amiri, H., Aminy, M., Lotfi, M., and Jafarbeglo, B., 2021, "Energy and Exergy Analysis of a New Solar Still Composed of Parabolic Trough Collector With Built-in Solar Still," Renewable Energy, **163**, pp. 465–479.
[13] Younis, M., Habchi, C., Ahmad, M. N., and Ghali, K., 2020, "Optimization of the Performance of a Solar Still Assisted by a Rotating Drum With a Rough Surface," Sol. Energy, **211**, pp. 847–865.
[14] Saravanan, A., and Murugan, M., 2020, "Performance Evaluation of Square Pyramid Solar Still With Various Vertical Wick Materials—An Experimental Approach," Therm. Sci. Eng. Prog., **19**, p. 100581.
[15] Murugan, M., Saravanan, A., Murali, G., Kumar, P., and Reddy, V. S. N., 2021, "Enhancing Productivity of V-Trough Solar Water Heater Incorporated Flat Plate Wick-Type Solar Water Distillation System," ASME J. Heat Transfer, **143**(3), p. 032001.
[16] Dumka, P., Chauhan, R., and Mishra, D. R., 2020, "Experimental and Theoretical Evaluation of a Conventional Solar Still Augmented With Jute Covered Plastic Balls," J. Energy Storage, **32**, p. 101874.
[17] Murugan, M., Saravanan, A., Kumar, P., Siva Nagi Reddy, V., and Arif, A., 2021, "An Overview About Influence of Wick Materials on Heat and Mass Transfer in Solar Desalination Systems," IOP Conf. Ser. Mater. Sci. Eng., **1057**(1), p. 012044.
[18] Alshammari, F., Elashmawy, M., and Ahmed, M. M. Z., 2021, "Cleaner Production of Freshwater Using Multi-Effect Tubular Solar Still," J. Clean. Prod., **281**, p. 125301.
[19] Yan, T., Xie, G., Liu, H., Wu, Z., and Sun, L., 2020, "CFD Investigation of Vapor Transportation in a Tubular Solar Still Operating Under Vacuum," Int. J. Heat Mass Transfer, **156**, p. 119917.
[20] Kabeel, A. E., Harby, K., Abdelgaied, M., and Eisa, A., 2020, "Augmentation of a Developed Tubular Solar Still Productivity Using Hybrid Storage Medium and CPC: An Experimental Approach," J. Energy Storage, **28**, p. 101203.
[21] Kabeel, A. E., Harby, K., Abdelgaied, M., and Eisa, A., 2020, "Performance of the Modified Tubular Solar Still Integrated With Cylindrical Parabolic Concentrators," Sol. Energy, **204**, pp. 181–189.
[22] Sathyamurthy, R., Mageshbabu, D., Madhu, B., Muthu Manokar, A., Rajendra Prasad, A., and Sudhakar, M., 2020, "Influence of Fins on the Absorber Plate of Tubular Solar Still—An Experimental Study," Mater. Today Proc., **46**(9), pp. 3270–3274.
[23] Abdelgaied, M., Harby, K., and Eisa, A., 2021, "Performance Improvement of Modified Tubular Solar Still by Employing Vertical and Inclined Pin Fins and External Condenser: An Experimental Study," Environ. Sci. Pollut. Res., **28**(11), pp. 13504–13514.
[24] Kabeel, A. E., Abdelgaied, M., Harby, K., and Eisa, A., 2020, "Augmentation of Diurnal and Nocturnal Distillate of Modified Tubular Solar Still Having Copper Tubes Filled With PCM in the Basin," J. Energy Storage, **32**, p. 101992.
[25] Kabeel, A. E., Sathyamurthy, R., Manokar, A. M., Sharshir, S. W., Essa, F. A., and Elshiekh, A. H., 2020, "Experimental Study on Tubular Solar Still Using Graphene Oxide Nano Particles in Phase Change Material (NPCM's) for Fresh Water Production," J. Energy Storage, **28**, p. 101204.
[26] Tiwari, G. N., and Kumar, A., 1988, "Nocturnal Water Production by Tubular Solar Stills Using Waste Heat to Preheat Brine," Desalination, **69**(3), pp. 309–318.
[27] Kabeel, A. E., Sharshir, S. W., Abdelaziz, G. B., Halim, M. A., and Swidan, A., 2019, "Improving Performance of Tubular Solar Still by Controlling the Water Depth and Cover Cooling," J. Clean. Prod., **233**, pp. 848–856.
[28] Abdullah, A. S., Omara, Z. M., Essa, F. A., Younes, M. M., Shanmugan, S., Abdelgaied, M., Amro, M. I., Kabeel, A. E., and Farouk, W. M., 2021, "Improving the Performance of Trays Solar Still Using Wick Corrugated Absorber, Nano-Enhanced Phase Change Material and Photovoltaics-Powered Heaters," J. Energy Storage, **40**, p. 102782.
[29] Abdelgaied, M., Zakaria, Y., Kabeel, A. E., and Essa, F. A., 2021, "Improving the Tubular Solar Still Performance Using Square and Circular Hollow Fins With Phase Change Materials," J. Energy Storage, **38**, p. 102564.
[30] Kumar, A., and Anand, J. D., 1992, "Modelling and Performance of a Tubular Multiwick Solar Still," Energy, **17**(11), pp. 1067–1071.
[31] Kabeel, A. E., Harby, K., Abdelgaied, M., and Eisa, A., 2021, "Performance Improvement of a Tubular Solar Still Using V-Corrugated Absorber With Wick Materials: Numerical and Experimental Investigations," Sol. Energy, **217**, pp. 187–199.
[32] Abdullah, A. S., Essa, F. A., Omara, Z. M., Rashid, Y., Hadj-Taieb, L., Abdelaziz, G. B., and Kabeel, A. E., 2019, "Rotating-Drum Solar Still With Enhanced Evaporation and Condensation Techniques: Comprehensive Study," Energy Convers. Manage., **199**, p. 112024.
[33] Essa, F. A., Abdullah, A. S., and Omara, Z. M., 2021, "Improving the Performance of Tubular Solar Still Using Rotating Drum—Experimental and Theoretical Investigation," Process Saf. Environ. Prot., **148**, pp. 579–589.
[34] Holman, J. P., 1978, *Experimental Methods For Engineers*, McGraw-Hill, New York.
[35] Gericke, A., and Van der Pol, J., 2010, "A Comparative Study of Regenerated Bamboo, Cotton and Viscose Rayon Fabrics. Part 1: Selected Comfort Properties," J. Fam. Ecol. Consum. Sci., **38**(1), pp. 63–73.
[36] WHO, 2017, *Guidelines for Drinking-Water Quality, 4th Edition, Incorporating the 1st Addendum*, World Health Organization, Geneva.